bioRxiv preprint doi: https://doi.org/10.1101/2020.01.22.915330; this version posted January 23, 2020. The copyright holder for this preprint (which was not certified by peer review) is the author/funder, who has granted bioRxiv a license to display the preprint in perpetuity. It is made available under aCC-BY-NC-ND 4.0 International license.

Disentangling the roles of neocortical alpha/beta and hippocampal theta/gamma activity in human episodic memory

Benjamin J. Griffiths[1,2], María Carmen Martín-Buro[3,4], Bernhard P. Staresina[1,2], & Simon Hanslmayr[1,2]

1) School of Psychology, University of Birmingham, UK
2) Centre for Human Brain Health, University of Birmingham, UK
3) Laboratory of Cognitive and Computational Neuroscience (UCM-UPM), Center for Biomedical Technology, 28223 Pozuelo de Alarcón, Madrid, Spain
4) Faculty of Health Sciences, King Juan Carlos University, 28922 Alcorcón, Madrid, Spain

Contact Information / Corresponding Author

Simon Hanslmayr

s.hanslmayr@bham.ac.uk

+44 121 4146203

Manuscript details

Number of pages:	18
Number of figures:	4
Abstract word count:	200
Introduction word count:	590
Discussion word count:	1,150

Preregistration available at: https://osf.io/4nt23/ (also included in supplementary materials).

Data available at: TBC

Code available at: https://github.com/benjaminGriffiths/dissociable_markers_of_memory.

Conflict of interest

The authors declare no competing financial interests.

bioRxiv preprint doi: https://doi.org/10.1101/2020.01.22.915330; this version posted January 23, 2020. The copyright holder for this preprint (which was not certified by peer review) is the author/funder, who has granted bioRxiv a license to display the preprint in perpetuity. It is made available under aCC-BY-NC-ND 4.0 International license.

Abstract

Episodic memory relies on two processes: 1) our ability to process a vast amount of sensory information, and 2) our ability to bind these sensory representations together to form a coherent memory. The first process is thought to rely on neocortical alpha/beta desynchronisation while the second is thought to be supported by hippocampal theta and gamma synchronisation. However, recent empirical evidence suggests that these two neural phenomena are contingent on one another, questioning whether alpha/beta desynchronisation and theta/gamma synchronisation truly reflect distinct processes. Here, we addressed this conundrum by asking seventeen participants to complete a paradigm that temporally separated sensory information representation and mnemonic binding while undergoing MEG recordings. We found that, during the perception and retrieval of task-relevant information, neocortical alpha/beta power monotonically decreased with the number of items recalled from a sequence. During mnemonic binding however, hippocampal theta/gamma phase-amplitude coupling monotonically increased with the number of sequence items later recalled. These results suggest a double dissociation between neocortical alpha/beta and hippocampal theta/gamma activity, with alpha/beta desynchronisation uniquely relating to information representation and theta/gamma phase-amplitude coupling uniquely relating to mnemonic binding. As such, we conclude that alpha/beta desynchronisation and hippocampal theta/gamma synchronisation represent two separable processes in episodic memory.

Significance Statement

Episodic memories are highly detailed snapshots of our personally experienced past. The formation and retrieval of episodic memories have consistently been shown to rely on the hippocampus and the sensory neocortex. However, it is unknown whether the memory-related neural activity in the hippocampus and neocortex reflect separate, interacting cognitive processes, or are two neural responses to a singular process. Here, we find evidence in favour of the former. Memory-related decreases in neocortical alpha/beta power uniquely arise to the perception and retrieval of event-related information, while memory-related increases in hippocampal theta/gamma phase-amplitude coupling uniquely arise during mnemonic binding. This double dissociation suggests that the neocortex and hippocampus play distinct and separable roles in the formation and retrieval of episodic memories

Introduction

An episodic memory is a detail-rich, long-term memory that is anchored to a unique point in time and space (Tulving, 2002). The formation and retrieval of these memories are thought to rely on neocortical alpha/beta desynchronisation and hippocampal theta/gamma synchronisation (Hanslmayr, Staresina, & Bowman, 2016), both of which are prevalent in a wide range of episodic memory tasks (for reviews, see Hanslmayr & Staudigl, 2014; Nyhus & Curran, 2010).

bioRxiv preprint doi: https://doi.org/10.1101/2020.01.22.915330; this version posted January 23, 2020. The copyright holder for this preprint (which was not certified by peer review) is the author/funder, who has granted bioRxiv a license to display the preprint in perpetuity. It is made available under aCC-BY-NC-ND 4.0 International license.

Neocortical alpha/beta desynchrony is thought to be beneficial for information representation (Hanslmayr, Staudigl, & Fellner, 2012). This idea is derived from the tenets of information theory, which propose that unpredictable states (e.g. a desynchronised network, where the firing of one neuron cannot predict the firing of another) can convey substantially more information than predictable states. In support of this idea, a recent EEG-fMRI study demonstrated that the amount of stimulus-specific information present in BOLD signal can be predicted by neocortical alpha/beta power (Griffiths, Mayhew, et al., 2019), suggesting that alpha/beta power directly correlates with neocortical information representation. Moreover, interfering with these power decreases via transcranial brain stimulation impairs both episodic memory formation and retrieval (Hanslmayr, Matuschek, & Fellner, 2014; Waldhauser, Braun, & Hanslmayr, 2016), suggesting that these power decreases play a causal role in memory. Based on these findings (and others; e.g. Fellner, Bäuml, & Hanslmayr, 2013; Long & Kahana, 2015; Sederberg et al., 2007), one can hypothesise that alpha/beta power decreases relate to the representation of information in episodic memory.

Hippocampal theta/gamma synchrony also correlates with episodic memory formation and retrieval. A memory-related increase in synchronisation can take the form of an increase in theta or gamma power (e.g. Burke et al., 2013; Griffiths, Parish, et al., 2019; Long & Kahana, 2015; Montgomery & Buzsáki, 2007; Osipova et al., 2006; Sederberg et al., 2007; Staresina et al., 2016), or an increase in the coupling between these two oscillations (e.g. Bahramisharif, Jensen, Jacobs, & Lisman, 2018; Heusser, Poeppel, Ezzyat, & Davachi, 2016; Staudigl & Hanslmayr, 2013; Tort, Komorowski, Manns, Kopell, & Eichenbaum, 2009). Mechanistically speaking, an increase in hippocampal synchronisation is thought to facilitate the binding of information into a coherent memory trace (Hanslmayr et al., 2016; Nyhus & Curran, 2010). This is, in part, dictated by theta phase, which determines whether long-term potentiation (LTP) or long-term depression (LTD) occurs (Hasselmo, Bodelón, & Wyble, 2002). Gamma synchronisation compliments this process by driving neurons to fire at the frequency optimal for spike-timing dependent plasticity (STDP; Bi & Poo, 1998; Jutras, Fries, & Buffalo, 2009; Nyhus & Curran, 2010). By coupling gamma power to the phase of theta that is optimal for LTP, the propensity for mnemonic binding is further enhanced.

However, hippocampal activation during encoding is contingent on the amount of preceding neocortical desynchronisation, and vice versa during episodic memory retrieval (Griffiths, Parish, et al., 2019). Statistically speaking, it is therefore plausible to suggest that a single latent variable produces both neocortical desynchronisation and hippocampal synchronisation. Here, we tested this idea using a paradigm that temporally separates information representation and mnemonic binding. If neocortical desynchronisation and hippocampal synchronisation reflect distinct cognitive processes, we would therefore expect that (1) neocortical alpha/beta power decreases are most prevalent during periods of information representation, and (2) hippocampal theta/gamma power increases and phase-amplitude coupling are most prevalent during mnemonic binding. Foreshadowing the results presented below, we find evidence to suggest that occipital

bioRxiv preprint doi: https://doi.org/10.1101/2020.01.22.915330; this version posted January 23, 2020. The copyright holder for this preprint (which was not certified by peer review) is the author/funder, who has granted bioRxiv a license to display the preprint in perpetuity. It is made available under aCC-BY-NC-ND 4.0 International license.

alpha/beta power decreases uniquely accompany sensory information representation, while increases in hippocampal theta-gamma coupling uniquely accompany mnemonic binding. These results reveal a double dissociation between neocortical alpha/beta desynchrony and hippocampal theta/gamma synchrony in episodic memory.

Materials and Methods

Participants

Twenty-eight participants were recruited (mean age = 25.4; age range = 20-33; 68% female; 82% right-handed). In return for their participation, they received course credit or financial reimbursement. One participant was excluded for excessive head movement (greater than 2 standard deviations above group mean). Four participants were excluded for poor quality data (more than 50% of trials rejected for artifacts). Six participants were excluded for poor memory performance (fewer than 15 trials in one of the three memory conditions). All exclusion criteria were pre-registered (see https://osf.io/4nt23/; see supplementary materials). This left seventeen participants for further analysis. Ethical approval was granted by the Research Ethics Committee at the University of Birmingham (ERN_15-0335), complying with the Declaration of Helsinki.

Experimental design

Each participant completed a visual associative memory task (see figure 1a). During encoding, participants were presented with a line drawing of an object, a pattern, and a scene (each for 1500ms, with a 500ms fixation cross shown between each stimulus). The order in which the pattern and scene were presented was swapped between each block (where a "block" is defined as a complete cycle of encoding, distractor and retrieval tasks). A prompt then appeared on screen instructing the participants to vividly associate these three items for a later memory test. Participants were then asked how difficult they found associating the triad. This question was used to keep participants attending to the task, rather than provide a meaningful metric for analysis. The next trial began after the participant had responded to the difficulty question. After associating 48 triads, participants started the distractor task. In the distractor task, participants attended to a fixation cross in the centre of a black screen. The fixation cross would flash from light grey to either white or dark grey momentarily (~100ms) approximately every 20 seconds. The participants were instructed to count the number of times the fixation cross changed to white (ignoring the times it turned dark grey) and report this value at the end of the task (approximately 2.5mins later). The retrieval task followed the distractor. Here, participants were presented with the line drawing and asked to recall the association they made earlier. After 3000ms, participants were presented with three patterns (one correct and two lures) to select from. After responding, participants were presented with three scenes (one correct and two lures). On blocks where scenes preceded patterns during perception, the presentation order at retrieval was also reversed. After responding, participants were then asked to indicate how confident they were about their choices. They could select 'guess' (i.e. they guessed their choice), 'unsure' (i.e. they could not remember the item, but had a feeling

bioRxiv preprint doi: https://doi.org/10.1101/2020.01.22.915330; this version posted January 23, 2020. The copyright holder for this preprint (which was not certified by peer review) is the author/funder, who has granted bioRxiv a license to display the preprint in perpetuity. It is made available under aCC-BY-NC-ND 4.0 International license.

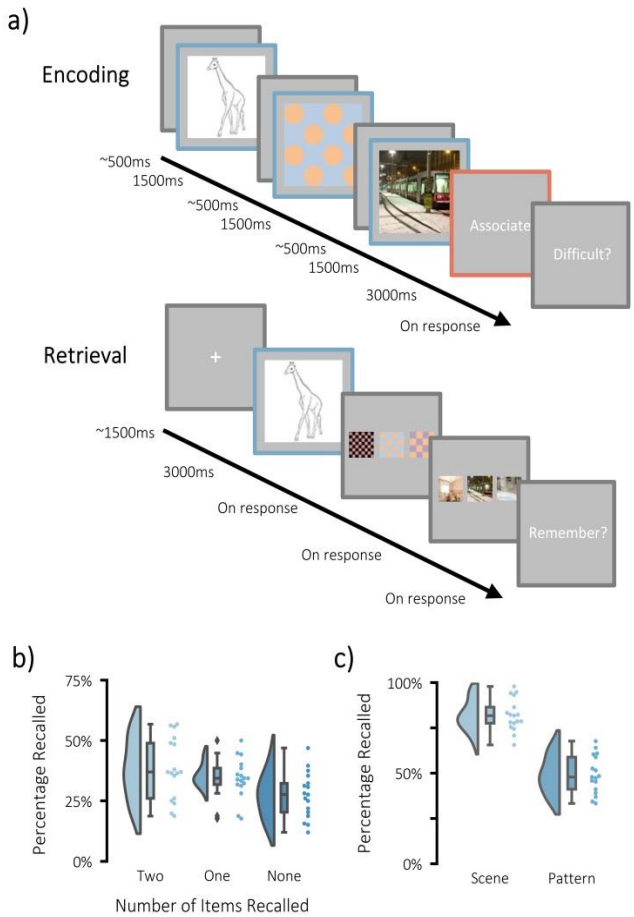

Figure 1. Overview of behavioural task. (a) Paradigm schematic. Participants were presented with a sequence of three visual stimuli. The sequence always began with a line drawing of an object, and was then followed by a pattern and a scene (each with a brief fixation cross shown between). Participants were then given a short interval to create a mental image incorporating the three stimuli. They were then asked to rate how plausible they found the mental image they created. After a distractor task, participants were presented with the object as a cue and asked to recall both the pattern and the scene, each from a choice of three stimuli. After selection, participants had to rate how confident they felt about their response. Windows of information processing are outlined in blue, and windows of mnemonic binding are outlined in red (b) Raincloud plot depicting memory performance for each participant. (c) Raincloud plot depicting memory performance for each stimulus type. Scene stimuli were better recalled than pattern stimuli.

it was the correct choice), or 'certain' (i.e. they could vividly remember the item). Participants were asked to recall all 48 triads learnt in the earlier encoding phase. Participants completed 4 blocks of this task (192 trials in total).

Behavioural analysis

For each trial, memory performance was coded as either 'complete' (i.e. they remembered both the scene and the pattern), 'partial' (i.e. they remembered only one of the associates), or 'forgotten' (i.e. they remembered neither the scene nor the pattern). Any trial where the participant indicated that they guessed was marked as a 'miss'. A dependent-samples t-test was used to contrast recall performance for patterns versus scenes.

MEG acquisition

MEG data was recorded using a 306-channel (204 gradiometers, 102 magnetometers) whole brain Elekta Neuromag TRIUX system (Elekta, Stockholm, Sweden) in a magnetically shielded room. Participants were placed in the supine position for the duration of the experiment. Data was continuously recorded at a sampling rate of 1000Hz. The headshape of each participant (including nasion and left/right ear canal) was digitised prior to commencing the experiment. Continuous head position indicators (cHPI) were recorded throughout. The frequencies emitted by the cHPI coils were 293Hz, 307Hz, 314Hz and 321Hz. Magnetometer data was excluded from the main analysis as they contained substantial noise that could not be effectively removed or attenuated.

MEG preprocessing

All data analysis was conducted in Matlab using Fieldtrip (Oostenveld, Fries, Maris, & Schoffelen, 2011) in conjunction with custom scripts. First, the data was low-pass filtered at 165Hz to remove the signal generated by the HPI coils. Second, the data was epoched around each event of interest. At encoding, the epochs reflected the time windows where each stimulus was presented (from here on termed 'perception') and when the 'associate' prompt was presented (termed 'association'). At retrieval, the epochs reflected the time window when the object cue was presented

bioRxiv preprint doi: https://doi.org/10.1101/2020.01.22.915330; this version posted January 23, 2020. The copyright holder for this preprint (which was not certified by peer review) is the author/funder, who has granted bioRxiv a license to display the preprint in perpetuity. It is made available under aCC-BY-NC-ND 4.0 International license.

(termed 'retrieval'). Perception epochs began 2000ms before stimulus onset and ended 3500ms after onset (that is, 2000ms after stimulus offset). Association and retrieval epochs began 2000ms before stimulus onset and ended 4500ms after onset (that is, 2000ms after stimulus offset). Third, independent components analysis was conducted, and any identifiable eye-blink or cardiac components were removed. Fourth, the data was visually inspected and any artefactual epochs or sensors were removed from the dataset (mean percentage of trials removed: 18.0%; range: 5.7-32.2%).

Movement correction

To identify participants with extreme head motion during MEG recordings, the recorded data was first high-pass filtered to 250Hz to isolate the cHPI signal. Second, the variance of the signal for each sensor was computed across every time point of the continuous recording. Third, the variance was mean averaged across sensors to provide a singular estimate of change in cHPI signal across the duration of the experiment. Fourth, the mean variance and its standard deviation was calculated across participants. Lastly, participants with extreme head motion were identified as those with variance greater than two standard deviations above the group mean. These participants were excluded from further analysis.

To help attenuate motion-related confounds in the spectral power analyses, a trial-by-trial estimate of motion was calculated. First, the data was high-pass filtered at 250Hz. Second, the data was epoched into trials matching those outlined in the section above. Third, the envelope of the signal in each epoch was then calculated (to avoid issues of mean phase angle difference in cHPI signal across trials). Fourth, the envelope was averaged over time to provide a single value for each epoch and channel. Fifth, the dot product was computed across sensors between the first epoch and every other epoch (algebraically: $\sum_{i=1}^{n} a_i\, b_i$, where *n* is the number of channels, a_i is the power at sensor *i* during the first trial, and b_i is the power at sensor *i* during the trial of interest). This provided a single value (between zero and infinity) for each trial that described how similar the topography of that trial was to the first trial – the higher the value, the more similar the topographies are between the two trials (with the assumption that the more dissimilar a cHPI topography is to the starting topography, the more the head has deviated from its starting position). These values were entered as a regressor of no interest in the central multiple regression analyses.

Time-frequency decomposition and statistical analysis

Sensor-level time-frequency decomposition was conducted on the three epochs (perception, association, and retrieval). For low frequencies, the preprocessed data was first convolved with a 6-cycle wavelet (-0.5 to 3 seconds, in steps of 50ms; 2 to 40Hz; in steps of 1Hz). For high frequencies, Slepian multitapers were first used to estimate power (-0.5 to 3 seconds, in steps of 50ms; 40 to 100Hz, in steps of 4Hz). For this latter analysis, frequency smoothing was set to one quarter of the frequency of interest and temporal smoothing was set to 200ms. Second, planar gradiometers were combined by summing the power of the vertical and horizontal components. Third, for perceptual trials only, power was then averaged over the three stimulus presentation windows of each triad to provide mean power during perception of the triad. Any triads where one or more epochs had been rejected during preprocessing were excluded at this stage. Fourth, the data was baseline correlated by means of z-transformation (Griffiths et al., 2016). To this end, power was first averaged over time for each trial, channel and frequency band. The mean and standard deviation of this time-averaged power was then computed across trials. This mean was then subtracted from power for each trial, and the resulting value was divided by the standard deviation.

bioRxiv preprint doi: https://doi.org/10.1101/2020.01.22.915330; this version posted January 23, 2020. The copyright holder for this preprint (which was not certified by peer review) is the author/funder, who has granted bioRxiv a license to display the preprint in perpetuity. It is made available under aCC-BY-NC-ND 4.0 International license.

For statistical analysis, a multiple regression was run for each participant using four regressors to predict observed power within a channel x frequency x time point. These four regressors were (1) number of items recalled, (2) whether the scene was recalled, (3) whether the pattern was recalled, (4) the change in head position [based on the motion calculation outlined above]. The first regressor was of primary interest, while the others were used to account for variance from potentially confounding sources. The beta weight of the first regressor, obtained for a given channel x frequency x time point, was then transformed into a t-value (by dividing by the standard error) to attenuate the impact of poor model fits on the final analysis. Here, a positive t-value would indicate that spectral power increases with more items recalled, and a negative t-value would indicate that spectral power decreases with more items recalled. The t-values for each participant were pooled across the sample and entered into a one-sample t-test to examine whether the observed fits consistently deviated from the null hypothesis (t=0) across participants. To address the issue of multiple comparisons, the t-values were subjected to a one-tailed cluster-based permutation test (2000 permutations; Maris & Oostenveld, 2007). Clusters that produced a p-value less than 0.05 were considered significant.

Model comparison

Notably, several statistical patterns can produce an apparent linear effect of memory performance. To examine the statistical pattern that produce the result observed in our multiple regression analyses, we generated three models that could, theoretically, produce such a trend:

Monotonic model: A monotonic trend where power decreases with increasing memory performance. Here, complete memories were coded with the value 2, partial memories with the value 1, and forgotten triads were coded with the value 0.

Hit vs. miss model: A binary division where any successful encoding produces a power decrease relative to the forgotten triads, but no distinction exists between triads that were completely recalled and triads that were only partially recalled. Here, complete and partial memories were coded with the value 1, and forgotten triads were coded with the value 0.

All-or-nothing model: A binary division where any successful encoding of the entire triad produces a power decrease relative to the partial and forgotten triads, but no distinction exists between triads that were partially recalled and triads that were forgotten (the "all-or-nothing model"). Here, complete memories were coded with the value 1, and partial and forgotten triads were coded with the value 0.

The first of these predictors matches that described in the 'time-frequency analysis' section. The multiple regression outlined in that section was re-run using the latter two models described above. As the monotonic model is the linear sum of the hit vs. miss model and the all-or-nothing model, this creates rank deficiency in the predictor matrix. Therefore, separate solutions for the three models had to be calculated. The effect size [Cohen's d_z; where $d_z = t / \mathrm{sqrt}(n)$, and n = number of participants] of the maximum cluster identified in the main text was calculated for each model. The model which produced the greatest effect size was interpreted as the model which best fit the data.

Source analysis

The preprocessed data was reconstructed in source space using individual head models and structural (T1-weighted) MRI scans for all but two individuals who did not wish to return for an MRI scan. For these two individuals, a standard head

bioRxiv preprint doi: https://doi.org/10.1101/2020.01.22.915330; this version posted January 23, 2020. The copyright holder for this preprint (which was not certified by peer review) is the author/funder, who has granted bioRxiv a license to display the preprint in perpetuity. It is made available under aCC-BY-NC-ND 4.0 International license.

model and MRI scan was used (taken from the Fieldtrip toolbox; for details, see http://www.fieldtriptoolbox.org/template/headmodel). The headshape (together with the HPI coil positions) of each participant was digitised using a Polhemus Fasttrack system. The timelocked MEG data was reconstructed using a single-shell forward model and a Linearly Constrained Minimum Variance beamformer (LCMV; van Veen, van Drongelen, Yuchtman, & Suzuki, 1997). The lambda regularisation parameter was set to 1%.

1/f correction

To isolate oscillatory contributions, 1/f activity was attenuated in the time-frequency data by subtracting the linear fit of 1/f characteristic (Griffiths, Parish, et al., 2019; Manning, Jacobs, Fried, & Kahana, 2009; Zhang & Jacobs, 2015). To this end, a vector containing values of each derived frequency (*A*) and another vector containing the power spectrum, averaged over all time-points and trials of the relevant memory condition, (*B*) were log-transformed at approximate a linear function. The linear equation $Ax = B$ was solved using least-squares regression, where x is an unknown constant describing the curvature of the 1/f characteristic. The 1/f fit (Ax) was then subtracted from the log-transformed power spectrum (*B*). As this fit can be biased by outlying peaks (Haller et al., 2018), an iterative algorithm was used that removed probable peaks and then refitted the 1/f. Outlying peaks in this 1/f-subtracted power spectrum were identified using a threshold determined by the mean value of all frequencies that sat below the linear fit. The MEG power spectrum is the summation of the 1/f characteristic and oscillatory activity (i.e. at no point does oscillatory activity subtract from the 1/f), therefore all values that sit below the linear fit can be seen an error of the fit. Any peaks that exceed the threshold were removed from the general linear model, and the fitting was repeated. Notably, as power for the low frequencies (2-40Hz) and high frequencies (40-100Hz) was calculated using different methods (wavelets and DPSS multitapers, respectively), the two bands have disparate levels of temporal and spectral smoothing. To avoid a spurious fitting due of the 1/f because of these differences, the 1/f correction was conducted separately for these two bands.

MEG phase-amplitude coupling computation and statistical analysis

To calculate the extent to which hippocampal gamma activity coupled to hippocampal theta phase, the modulation index (MI) was calculated (Tort et al., 2010). First, the peak theta and gamma frequencies were calculated by estimating power across all hippocampal virtual sensors (bilaterally, as defined by the automated anatomical labelling [AAL] atlas) using the same time-frequency decomposition method reported above. The Matlab function *findpeaks()* was then used to extract the most prominent peak within the theta (2-7Hz) and gamma (40-100Hz) bands for each participant. Across participants, the mean theta peak was at 5.0Hz, and the mean gamma peak was at 67.0Hz. Second, the time-series of the hippocampal virtual sensors were duplicated, with the first being filtered around the theta peak (±0.5Hz) and the second being filtered around the gamma peak (±5Hz). Third, the Hilbert transform was applied to the theta- and gamma-filtered time-series, with the phase of the former and power of the latter being extracted. Fourth, the time-series data was re-epoched, beginning 500ms after the onset of the stimulus/fixation cross and ending 500ms before the onset of the next screen. This attenuated the possibility that an event-related potential and/or edge artifacts from the filtering/Hilbert transform could influence the phase-amplitude coupling measure (Aru et al., 2014). Fifth, gamma power was binned into 12 equidistant bins of 30°, according to the concurrent theta phase. This binning was conducted for each trial and sensor separately. Notably, as differences in trial number can bias the phase-amplitude coupling estimate, trial numbers for each memory condition were balanced. This was achieved by identifying the condition with the smallest number of trials and

bioRxiv preprint doi: https://doi.org/10.1101/2020.01.22.915330; this version posted January 23, 2020. The copyright holder for this preprint (which was not certified by peer review) is the author/funder, who has granted bioRxiv a license to display the preprint in perpetuity. It is made available under aCC-BY-NC-ND 4.0 International license.

then taking a matching number of trials from the other conditions (evenly distributed across the duration of the experiment). Sixth, the MI was computed by comparing the observed distribution to a uniform distribution. Seventh, the resulting MI values were subjected to a multiple regression conducted in the same manner as for the spectral power analyses. However, two additional regressors were added to this model: (1) hippocampal peak theta power [per trial, averaged across 500ms to 2500ms], (2) hippocampal peak gamma power [per trial, averaged across 500ms to 2500ms]. These regressors addressed the potential confound of concurrent power influence phase estimates (Aru et al., 2014). Eighth, these results were subjected to the same statistical procedure as outlined above; namely, a one-sample t-test comparing per-participant t-values relating phase-amplitude coupling to changes in memory performance to the null hypothesis (t=0).

To test the spatial specificity of this effect, the same pipeline was used to assess theta-gamma phase-amplitude coupling in the frontal, occipital, parietal and temporal lobes (individually; defined in by in *wfupickatlas* toolbox for SPM)

Results

Behavioural results

Participants, on average, correctly recalled both the associated pattern and associated scene on 38.3% of trials, recalled only one associated stimulus on 34.4% of trials, and failed to recall either associate on 27.3% of trials (see figure 1b). Participants correctly recalled the associated pattern on 49.2% of trials, and correctly recalled the associated scene on 82.1% of trials (both of which are well above chance performance [33.3%]; see figure 1c). A paired-samples t-test revealed that memory for scenes was substantially greater than memory for patterns ($p < 0.001$, Cohen's $d_z = 4.57$).

Occipital alpha/beta power decreases during stimulus perception predict successful memory formation

We first investigated the extent to which spectral power fluctuates as a function of memory performance during visual perception. We hypothesised that, as information surrounding the three stimuli needs to be processed in order to form a complete memory, alpha/beta power should monotonically decrease as a function of memory performance. To test this, the time-series of sensor-level MEG gradiometer data was decomposed into spectral power using 6-cycle Morlet wavelets (for low frequencies; 2-40Hz) and Slepian multitapers (for high frequencies; 40-100Hz), and then baseline-corrected using z-transformation on the artifact-free data. Spectral power was then entered as an outcome variable into a multiple regression with four predictor variables: the number of items recalled, whether the scene was recalled, whether the pattern was recalled, and head motion. The first regressor was of primary interest, while the latter three were used to attenuate potentially confounding variables. This returned a t-value (beta coefficient divided by standard error) for each participant. Here, a positive t-value would indicate that spectral power increases with the number of items recalled and a negative t-value would indicate that spectral power decreases with the number of items recalled. The t-values for each participant were pooled and entered into a group-level, cluster-based one-sample t-test

bioRxiv preprint doi: https://doi.org/10.1101/2020.01.22.915330; this version posted January 23, 2020. The copyright holder for this preprint (which was not certified by peer review) is the author/funder, who has granted bioRxiv a license to display the preprint in perpetuity. It is made available under aCC-BY-NC-ND 4.0 International license.

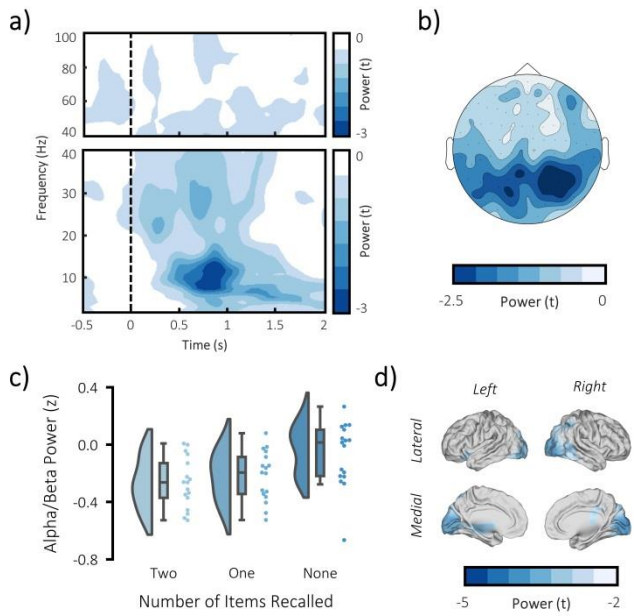

Figure 2. Alpha/beta power decreases during perception correlate with increased memory performance. (a) Time-frequency representation over occipital and parietal sensors shows that a decrease in low-frequency power (8-20Hz) correlates with later memory success. **(b)** A topographic plot of post-stimulus alpha/beta power suggests that memory-related power decreases were most prominent over the occipital lobe. **(c)** Raincloud plot depicting alpha/beta power as a function of items recalled. Power appeared to linearly decrease with greater memory performance. **(d)** Source reconstruction of this effect confirmed this, as well as implicating parts of the parietal lobe and ventral medial prefrontal cortex.

which compared observed values against the null hypothesis (t=0; Maris & Oostenveld, 2007). This analytical approach revealed a significant effect where power decreases correlated with an increase in memory performance (p_{corr} = 0.013, Cohen's d_z = 1.33). Visual inspection of the cluster suggests that the effect was greatest over the posterior sensors, bilaterally, between 8 and 20Hz (see figure 2a-b). The reconstruction of this effect on source level suggests that this effect primarily arose in the occipital lobe (see figure 2d).

It is important to note that three types of statistical patterns can produce the trend we uncovered: (1) a monotonic relationship where power decreases with increasing memory performance (the "monotonic model"), (2) a binary division where any successful encoding produces a power decrease relative to the forgotten triads, but no distinction exists between triads that were completely recalled and triads that were only partially recalled (the "hit vs. miss model"), and (3) a binary division where successful encoding of the entire triad produces a power decrease relative to the partial and forgotten triads, but no distinction exists between triads that were partially recalled and triads that were forgotten (the "all-or-nothing model"). To examine which model best fit the data, the effect size of each model was computed based on all data points found within the cluster. These values were then descriptively compared. It seemed the monotonic model best described the power decrease, producing an effect size of d_z = 1.33. The other models also produced large effect sizes (perhaps owning to the fact that they are very similar models) but, critically, they were smaller than the monotonic model (hit vs. miss: d_z = 1.25; all-or-nothing: d_z = 0.74). This suggests that alpha/beta power monotonically decreases with the amount of information encoded. It is worth considering that the decrease in alpha/beta power does not appear to be strictly linear (that is, the power decrease for one item recalled relative to no items recalled is not equivalent to the power decrease for two items recalled relative to one item). Rather, it'd appear that the difference in power is greater between one and no items recalled compared to two and one items recalled (see figure 2c). Therefore, we have refrained from referring to this effect (and indeed do not view this effect) as a "linear decrease" in power across

bioRxiv preprint doi: https://doi.org/10.1101/2020.01.22.915330; this version posted January 23, 2020. The copyright holder for this preprint (which was not certified by peer review) is the author/funder, who has granted bioRxiv a license to display the preprint in perpetuity. It is made available under aCC-BY-NC-ND 4.0 International license.

conditions. Rather, we choose to refer to this effect as "monotonically decreasing". That is, there is a decrease in power for one item recalled relative to no items, and a decrease in power for two items recalled relative to one, but these decreases are not equivalent.

Notably, the observed effect was spectrally broad. As such, it is reasonable to suggest that this effect may not reflect a change in oscillatory activity, but rather a change in the underlying 1/f characteristic (Haller et al., 2018; Miller, Sorensen, Ojemann, & Den Nijs, 2009). To address this, the 1/f characteristic of this cluster was isolated from the oscillatory signal by subtracting a linear fit of the 1/f characteristic in log-log space (see methods for details). This approach provides a power spectrum that describes memory-related changes in oscillatory power and a beta weight that describes the 1/f characteristic. Both measures were subjected to the same statistical analysis as above. This revealed a significant effect for oscillatory power ($p = 0.006$, Cohen's $d_z = 0.72$), where a decrease in alpha power (8-11Hz) correlated with an increase in memory performance. In addition, a trending effect was observed in the fractal slope, where a decrease in low frequency power and an increase in high frequency power correlated with greater memory performance ($p = 0.087$, Cohen's $d_z = 0.34$). A comparison of effect sizes suggests that a decrease in oscillatory alpha power is the primary driver of the monotonic relationship to memory performance.

Occipital and parietal alpha/beta power decreases during stimulus recall predict successful memory retrieval

We then asked how spectral power fluctuates as a function of memory performance during memory retrieval. We hypothesised that alpha/beta power should parametrically decrease as a function of memory performance, reflecting an increase in the representation of reinstated information. The analytical approach matched that reported above. In line with our hypothesis, we found a significant effect where post-stimulus alpha/beta power decreases correlated with an increase in memory performance ($p_{corr} = 0.025$, Cohen's $d_z = 1.32$; see figure 3a-b). Visual inspection of the cluster suggests that the effect was greatest over the frontal, and left parietal/occipital sensors, between 6-20Hz. Source reconstruction localised this effect to the parietal and retrosplenial cortices (see figure 3d). As during perception, it appeared that the linear model better account for the observed effect (Cohen's $d_z = 1.32$) rather than the hit vs. miss model (Cohen's $d_z = 1.26$) or the all-or-nothing model (Cohen's $d_z = 0.62$). Moreover, 1/f corrected analyses (conducted in the same manner as above) revealed a significant effect for oscillatory power ($p_{corr} = 0.002$; Cohen's $d_z = 0.72$), where a decrease in alpha/beta power (10-15Hz) correlated with an increase in memory performance. No significant cluster was observed for the beta weight describing the 1/f characteristic ($p = 0.323$, Cohen's $d_z = 0.14$). These results suggest that a decrease in oscillatory alpha/beta power, rather than a shift in 1/f, correlates with greater memory performance during successful memory retrieval.

bioRxiv preprint doi: https://doi.org/10.1101/2020.01.22.915330; this version posted January 23, 2020. The copyright holder for this preprint (which was not certified by peer review) is the author/funder, who has granted bioRxiv a license to display the preprint in perpetuity. It is made available under aCC-BY-NC-ND 4.0 International license.

Hippocampal theta/gamma phase-amplitude coupling during stimulus association predicts successful episodic memory formation

We then asked how spectral power fluctuates as a function of memory performance during the association window at encoding. We hypothesised that theta and gamma power should parametrically increase as a function of memory performance, reflecting an increase in hippocampal binding. The analytical approach matched that reported above. Intriguingly however, our analysis did not reveal any memory-related changes in theta or gamma power. As we had hypothesised that such effects would originate from the hippocampus, and deep sources can obscured by more superficial sources (Ruzich, Crespo-García, Dalal, & Schneiderman, 2019), we re-ran our analysis using a bilateral hippocampal region of interest, but still found no memory-related change in theta or gamma power. However, a trending effect in the alpha/beta frequency range was observed (p_{corr} = 0.059), where an increase in alpha/beta power correlated with enhanced memory performance. As this effect was not hypothesised and merely trending towards significance, we have relegated the analyses and discussion of this result to the supplementary information.

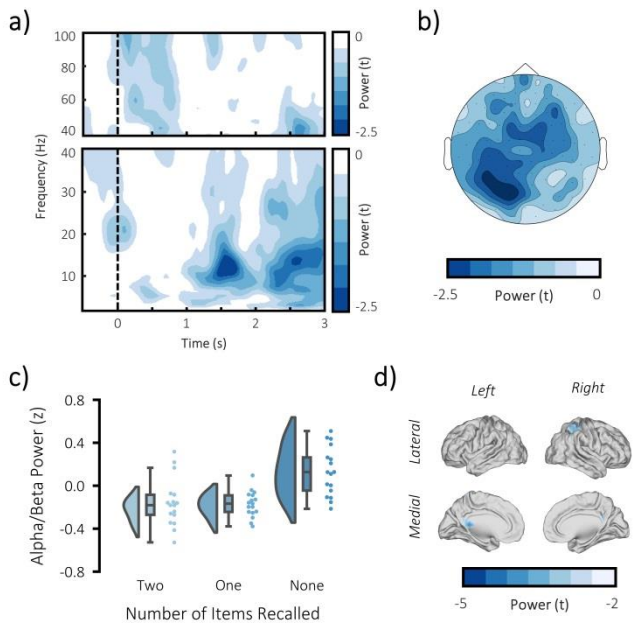

Figure 3. Alpha/beta power decreases during memory retrieval correlate with increased memory performance. **(a)** Time-frequency representation over left parietal sensors (top left) shows that a decrease in low-frequency power (8-20Hz) correlates with later memory success. **(b)** A topographic plot of post-stimulus alpha/beta power suggests the memory-related power decreases were most prominent over the left parietal and occipital regions. **(c)** Raincloud plot depicting power as a function of items recalled. Power appeared to decrease when successfully recalling a stimulus, but power did not vary as a function of the number of items recalled. **(d)** Source reconstruction of this effect (bottom right) confirmed this.

We then probed how theta/gamma phase-amplitude coupling relates to episodic memory formation and retrieval. To address this, we went straight to the source level as we had strong *a priori* hypotheses about the hippocampal source of this effect (see https://osf.io/4nt23/; see supplementary materials), and such a deep source can often be masked by more superficial sources (Ruzich et al., 2019). We first extracted the theta and gamma peaks in the hippocampal power spectrum for each participant individually. Across participants, the peak in hippocampal theta arose at 5.0Hz (when searching between 2 and 7Hz), while the peak hippocampal gamma frequency arose at 67.0Hz (when searching between 40 and 100Hz). By taking the peak frequencies, we ensured that analysis focused on the coupling between two oscillatory signals (Aru et al., 2014). Every sample of hippocampal gamma power was binned according to hippocampal theta phase, and the modulation index (Tort, Komorowski,

bioRxiv preprint doi: https://doi.org/10.1101/2020.01.22.915330; this version posted January 23, 2020. The copyright holder for this preprint (which was not certified by peer review) is the author/funder, who has granted bioRxiv a license to display the preprint in perpetuity. It is made available under aCC-BY-NC-ND 4.0 International license.

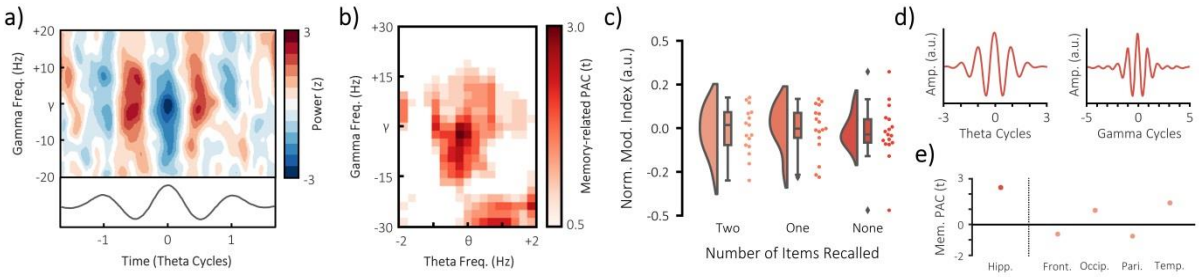

Figure 4. Increases in hippocampal theta/gamma coupling during mnemonic binding correlate with increased memory performance. (a) the modulation of peak gamma power as a function of peak theta phase across all trials. Peak gamma appears to decrease during the peaks of the theta phase, and increase during troughs of the theta phase. **(b)** the specificity of memory-related hippocampal theta-gamma phase-amplitude coupling. **(c)** raincloud plot depicting the fit between memory performance and hippocampal theta-gamma coupling (each dot represents a participant). **(d)** peak-locked average of peak theta (left) and gamma (right) frequencies, averaged across all participants. For both, theta and gamma the waveforms appear symmetric thus excluding a distortion of the cross-frequency coupling measure due to waveshape. **(e)** group-level t-statistic for the hippocampal region of interest compared to t-statistics for frontal, occipital, parietal and temporal regions of interest.

Eichenbaum, & Kopell, 2010) was computed for each trial (against the null hypothesis that the distribution of gamma power is uniform across the theta phase). The resulting modulation index values were then entered in a multiple regression (as described above) with the addition of two more nuisance regressors: concurrent theta power and concurrent gamma power. As power can affect the phase estimate, these regressors attenuate the potential influence of power on the trial-by-trial measures of PAC. These values were then entered into a one-sample t-test for statistical analysis in the same manner as above. During mnemonic binding, a significant increase in theta/gamma phase-amplitude coupling correlated with greater memory performance observed ($p = 0.012$, Cohen's $d_z = 0.61$; see figure 4). When examining which model best fit hippocampal phase-amplitude coupling, it appeared that the monotonic model of memory performance best described the effect (Cohen's $d_z = 0.61$; relative to hit vs. miss [Cohen's $d_z = 0.49$] and all-or-nothing [Cohen's $d_z = 0.43$] models). No significant coupling was observed during perception ($p = 0.500$, Cohen's $d_z < 0.01$) or retrieval ($p = 0.396$, Cohen's $d_z = 0.06$). These results suggest that memory-related theta/gamma phase-amplitude coupling is most prominent during periods of mnemonic binding.

To confirm the spatial specificity of the effect observed during mnemonic binding, we re-ran this analysis using four additional regions of interest: the frontal lobe, parietal lobe, temporal lobe (excluding the hippocampus), and the occipital lobe. None of these regions exhibited significant theta-gamma phase-amplitude coupling (frontal: $p = 0.308$, parietal: $p = 0.250$, temporal: $p = 0.078$, occipital: $p = 0.169$; see figure 4e). These results suggest the memory-related enhancement in theta/gamma phase-amplitude coupling predominately arises in the hippocampus.

bioRxiv preprint doi: https://doi.org/10.1101/2020.01.22.915330; this version posted January 23, 2020. The copyright holder for this preprint (which was not certified by peer review) is the author/funder, who has granted bioRxiv a license to display the preprint in perpetuity. It is made available under aCC-BY-NC-ND 4.0 International license.

Discussion

During episodic memory formation, the amount of hippocampal synchrony can be predicted by the amount of preceding neocortical desynchrony (Griffiths, Parish, et al., 2019). Similarly, the amount of neocortical desynchrony during episodic memory retrieval can be predicted by the preceding hippocampal synchrony. While this has been interpreted as the interaction between information representation within the neocortex and mnemonic binding in the hippocampus (Hanslmayr et al., 2016), such a correlation between two neural phenomena could also be ascribed to a singular latent variable. Here, we disentangle these two ideas by using a paradigm that temporally separated information representation and mnemonic binding. In this task, we found that memory-related decreases in neocortical alpha/beta power only arose during the perception and retrieval of the sequence, fitting with the idea that these decreases reflect information representation. In contrast, memory-related increases in hippocampal theta/gamma phase-amplitude coupling only arose during the association window, fitting with the idea that such coupling reflects the mnemonic binding of a memory. These results suggest that alpha/beta desynchronisation and hippocampal theta/gamma synchronisation reflect two distinct cognitive processes in episodic memory formation and retrieval.

The representation of information relating to an ongoing event or retrieved memory is thought to be supported by the desynchronisation of neocortical alpha/beta oscillations (Hanslmayr et al., 2012). Information theory proposes that unpredictable states carry more information than predictable states (Shannon & Weaver, 1949). As spiking in desynchronised neural networks is less predictable than spiking in synchronised networks, the former is thought to benefit information representation. Our findings add to the ever-increasing number of studies implicating neocortical alpha/beta power decreases in the successful formation and retrieval of episodic memories (e.g. Fell, Ludowig, Rosburg, Axmacher, & Elger, 2008; Fellner, Bäuml, & Hanslmayr, 2013; Griffiths et al., 2016; Hanslmayr et al., 2009, 2011; Long & Kahana, 2015; Sederberg et al., 2007; Waldhauser et al., 2016). Notably, our paradigm was sensitive to the amount of information encoded/retrieved. Therefore, it allowed us to ask if neocortical alpha/beta power decreases not only correlate with *whether* a memory is encoded/recalled or not (as investigated in the studies above), but *how much* of the memory is encoded/recalled. During perception and retrieval, our analysis suggests that alpha/beta power decreases directly correspond to the amount of information encoded about a memory. This result ties in with earlier findings which suggest that neocortical alpha/beta power decreases track the quantity of information reinstated within the brain (Griffiths, Mayhew, et al., 2019; Martín-Buro et al., 2019). Together, these results suggest that alpha/beta power has a monotonic relationship to the quantity of information being encoded and/or retrieved as an episodic memory.

We also investigated the role of hippocampal theta and gamma oscillations, with the hypothesis that synchronisation (both independently as power increases, and their conjunction in phase-amplitude coupling)

bioRxiv preprint doi: https://doi.org/10.1101/2020.01.22.915330; this version posted January 23, 2020. The copyright holder for this preprint (which was not certified by peer review) is the author/funder, who has granted bioRxiv a license to display the preprint in perpetuity. It is made available under aCC-BY-NC-ND 4.0 International license.

would monotonically increase with memory performance during the binding window. We were partially correct. We found that hippocampal theta-gamma phase-amplitude coupling scaled with memory performance – theta-gamma coupling monotonically increased with memory performance. Mechanistically speaking, these increases may reflect a heightened degree of long-term potentiation (LTP) within the hippocampus. By coupling gamma oscillations resonating at a frequency optimal for spike-timing dependent plasticity (STDP; Bi & Poo, 1998; Nyhus & Curran, 2010) to the phase of theta optimal for LTP (Hasselmo et al., 2002), the potential for building synaptic connections between hippocampal neurons is increased greatly. One could therefore speculate that the increase in theta-gamma coupling reflects an increase in underlying plasticity within the hippocampus. Alternatively, these increases in coupling may reflect enhanced representation of the sequence structure within the hippocampus. Numerous studies have suggested that theta-gamma phase-amplitude coupling provides an intricate mechanism well-suited for the representation and maintenance of sequences (Bahramisharif et al., 2018; Heusser et al., 2016; Lisman & Jensen, 2013) as well as complex event memories (Griffiths & Fuentemilla, 2019). Under these ideas, the observed increase in theta-gamma phase-amplitude coupling would be interpreted as reflecting a more robust representation of the sequence within the hippocampus, and perhaps this enhanced representation facilitates the encoding and retrieval of this sequence. Unfortunately, we cannot untangle these two ideas based on the data from the current paradigm. However, these two ideas needn't be adversarial. Indeed, sequence representation may be a convenient by-product of enhanced LTP via theta-gamma coupling, or vice versa. Regardless, it seems that hippocampal theta-gamma phase-amplitude coupling scales with the number of items recalled about a memory.

We did not observe any memory-related fluctuations in theta or gamma power during the binding window. We had been exploring theories that hippocampal theta/gamma synchronisation is beneficial for long-term potentiation (Bi & Poo, 1998; Hanslmayr et al., 2016; Nyhus & Curran, 2010), which emphasise the importance of theta phase for LTP, rather than power. Such theories would not anticipate that theta power would increase with enhanced mnemonic binding, perhaps explaining the absence of theta power fluctuations here. As increases in gamma power have been hypothesised to reflect increases in STDP, it is odd to not observe a strong increase in gamma power correlating with successful memory formation. However, our observed theta-gamma coupling effect may explain this. If memory-related increases in gamma power are restricted to particular phases of theta and theta is not stimulus-locked across trials, then across-trial averages of gamma power are unlikely to reveal any memory-related change as the temporal onset of these gamma power increases fluctuate across trials.

It is worth noting that we have, throughout this paper, considered information representation to arise solely during sequence perception and sequence retrieval, and mnemonic binding to arise solely during the binding window. However, it seems plausible to suggest these cognitive processes are not completely restricted to their respective windows. Indeed, one may anticipate that some processing of the stimulus arises during

bioRxiv preprint doi: https://doi.org/10.1101/2020.01.22.915330; this version posted January 23, 2020. The copyright holder for this preprint (which was not certified by peer review) is the author/funder, who has granted bioRxiv a license to display the preprint in perpetuity. It is made available under aCC-BY-NC-ND 4.0 International license.

mental association of the stimuli (Dijkstra, Bosch, & van Gerven, 2019), and that some mnemonic binding arises during sequence perception (Griffiths & Fuentemilla, 2019; Heusser et al., 2016). We do not dispute these ideas, but do suggest that any information representation that does arise during the binding window will be substantially smaller than the representation occurring during stimulus presentation, as we anticipate that the vast majority of stimulus processing to occur when participants are first shown the stimulus. Similarly, while some binding may arise during sequence perception, this will be substantially less than the binding that occurs at the end of the sequence, simply because any binding that arises before the end of the sequence has fewer stimuli to bind together. In short, while the two cognitive processes are unlikely to be completely segregated in this paradigm, there still is a substantial degree of segregation that allows us to investigate the distinct neural correlates of these processes.

In sum, we demonstrate that decreases in neocortical alpha/beta power and increases in hippocampal theta/gamma phase-amplitude coupling are functionally dissociable in episodic memory. These results add further support to the idea that neocortical desynchrony supports memory-related information representation while hippocampal synchrony supports mnemonic binding (Hanslmayr et al., 2016).

References

Aru, J., Priesemann, V., Wibral, M., Lana, L., Pipa, G., Singer, W., & Vicente, R. (2014). Untangling cross-frequency coupling in neuroscience. *Current Opinion in Neurobiology*, *31*(September 2014), 51–61. https://doi.org/10.1101/005926

Bahramisharif, A., Jensen, O., Jacobs, J., & Lisman, J. (2018). Serial representation of items during working memory maintenance at letter-selective cortical sites. *PLoS Biology*, 171660. https://doi.org/10.1101/171660

Bi, G., & Poo, M. (1998). Synaptic modifications in cultured hippocampal neurons: Dependence on spike timing, synaptic strength, and postsynaptic cell type. *Journal of Neuroscience*, *18*(24), 1–9. https://doi.org/10.1038/25665

Burke, J. F., Zaghloul, K. a., Jacobs, J., Williams, R. B., Sperling, M. R., Sharan, a. D., & Kahana, M. J. (2013). Synchronous and asynchronous theta and gamma activity during episodic memory formation. *Journal of Neuroscience*, *33*(1), 292–304. https://doi.org/10.1523/JNEUROSCI.2057-12.2013

Buzsáki, G., Anastassiou, C. A., & Koch, C. (2012). The origin of extracellular fields and currents-EEG, ECoG, LFP and spikes. *Nature Reviews Neuroscience*, *13*(6), 407–420. https://doi.org/10.1038/nrn3241

Dijkstra, N., Bosch, S. E., & van Gerven, M. A. J. (2019). Shared neural mechanisms of visual perception and imagery. *Trends in Cognitive Sciences*, *23*(5), 423–434. https://doi.org/10.1016/j.tics.2019.02.004

Fell, J., Ludowig, E., Rosburg, T., Axmacher, N., & Elger, C. E. (2008). Phase-locking within human mediotemporal lobe predicts memory formation. *NeuroImage*, *43*(2), 410–419. https://doi.org/10.1016/j.neuroimage.2008.07.021

Fellner, M.-C., Bäuml, K.-H. T., & Hanslmayr, S. (2013). Brain oscillatory subsequent memory effects differ in power and long-range synchronization between semantic and survival processing. *NeuroImage*, *79*, 361–370. https://doi.org/10.1016/j.neuroimage.2013.04.121

Fellner, M.-C., Gollwitzer, S., Rampp, S., Kreiselmeyr, G., Bush, D., Diehl, B., … Hanslmayr, S. (2019). Spectral fingerprints or spectral tilt? Evidence for distinct oscillatory signatures of memory formation. *PLOS Biology*, *17*(7), e3000403. https://doi.org/10.1371/journal.pbio.3000403

Griffiths, B. J., & Fuentemilla, L. (2019). Event conjunction: How the hippocampus integrates episodic memories across event boundaries. *Hippocampus*, 1–15. https://doi.org/10.1002/hipo.23161

Griffiths, B. J., Mayhew, S. D., Mullinger, K. J., Jorge, J., Charest, I., Wimber, M., & Hanslmayr, S. (2019). Alpha/beta power decreases

bioRxiv preprint doi: https://doi.org/10.1101/2020.01.22.915330; this version posted January 23, 2020. The copyright holder for this preprint (which was not certified by peer review) is the author/funder, who has granted bioRxiv a license to display the preprint in perpetuity. It is made available under aCC-BY-NC-ND 4.0 International license.

track the fidelity of stimulus-specific information. *ELife*, *8*(e49562), 1–22. https://doi.org/10.32470/ccn.2019.1199-0

Griffiths, B. J., Mazaheri, A., Debener, S., & Hanslmayr, S. (2016). Brain oscillations track the formation of episodic memories in the real world. *NeuroImage*, *143*, 256–266. https://doi.org/10.1101/042929

Griffiths, B. J., Parish, G., Roux, F., Michelmann, S., Plas, M. Van Der, Kolibius, D., … Hanslmayr, S. (2019). Directional coupling of slow and fast hippocampal gamma with neocortical alpha / beta oscillations in human episodic memory. *Proceedings of the National Academy of Sciences*, 1–9. https://doi.org/10.1073/pnas.1914180116

Haller, M., Donoghue, T., Peterson, E., Varma, P., Sebastian, P., Gao, R., … Voytek, B. (2018). Parameterizing neural power spectra. *BioRxiv*, 299859. https://doi.org/10.1101/299859

Hanslmayr, S., Matuschek, J., & Fellner, M.-C. (2014). Entrainment of prefrontal beta oscillations induces an endogenous echo and impairs memory formation. *Current Biology*, *24*(8), 904–909. https://doi.org/10.1016/j.cub.2014.03.007

Hanslmayr, S., Spitzer, B., & Bauml, K.-H. (2009). Brain oscillations dissociate between semantic and nonsemantic encoding of episodic memories. *Cerebral Cortex*, *19*(7), 1631–1640. https://doi.org/10.1093/cercor/bhn197

Hanslmayr, S., Staresina, B. P., & Bowman, H. (2016). Oscillations and episodic memory – Addressing the synchronization/desynchronization conundrum. *Trends in Neurosciences*, *39*(1), 16–25. https://doi.org/10.1016/j.tins.2015.11.004

Hanslmayr, S., & Staudigl, T. (2014). How brain oscillations form memories--a processing based perspective on oscillatory subsequent memory effects. *NeuroImage*, *85 Pt 2*, 648–655. https://doi.org/10.1016/j.neuroimage.2013.05.121

Hanslmayr, S., Staudigl, T., & Fellner, M.-C. (2012). Oscillatory power decreases and long-term memory: the information via desynchronization hypothesis. *Frontiers in Human Neuroscience*, *6*(74), 1–12. https://doi.org/10.3389/fnhum.2012.00074

Hanslmayr, S., Volberg, G., Wimber, M., Raabe, M., Greenlee, M. W., & Bauml, K.-H. T. (2011). The relationship between brain oscillations and BOLD signal during memory formation: A combined EEG-fMRI study. *Journal of Neuroscience*, *31*(44), 15674–15680. https://doi.org/10.1523/JNEUROSCI.3140-11.2011

Hasselmo, M. E., Bodelón, C., & Wyble, B. P. (2002). A proposed function for hippocampal theta rhythm: Separate phases of encoding and retrieval enhance reversal of prior learning. *Neural Computation*, *14*(4), 793–817. https://doi.org/10.1162/089976602317318965

Heusser, A. C., Poeppel, D., Ezzyat, Y., & Davachi, L. (2016). Episodic sequence memory is supported by a theta-gamma phase code. *Nature Neuroscience*, *19*(August). https://doi.org/10.1038/nn.4374

Jutras, M. J., Fries, P., & Buffalo, E. A. (2009). Gamma-Band Synchronization in the Macaque Hippocampus and Memory Formation. *Journal of Neuroscience*, *29*(40), 12521–12531. https://doi.org/10.1523/JNEUROSCI.0640-09.2009

Lisman, J. E., & Jensen, O. (2013). The theta-gamma neural code. *Neuron*, *77*(6), 1002–1016. https://doi.org/10.1016/j.neuron.2013.03.007

Long, N. M., & Kahana, M. J. (2015). Successful memory formation is driven by contextual encoding in the core memory network. *NeuroImage*, *119*, 332–337. https://doi.org/10.1016/j.neuroimage.2015.06.073

Manning, J. R., Jacobs, J., Fried, I., & Kahana, M. J. (2009). Broadband shifts in local field potential power spectra are correlated with single-neuron spiking in humans. *Journal of Neuroscience*, *29*(43), 13613–13620. https://doi.org/10.1523/JNEUROSCI.2041-09.2009

Maris, E., & Oostenveld, R. (2007). Nonparametric statistical testing of EEG- and MEG-data. *Journal of Neuroscience Methods*, *164*(1), 177–190. https://doi.org/10.1016/j.jneumeth.2007.03.024

Martín-Buro, M. C., Wimber, M., Henson, R. N., & Staresina, B. P. (2019). Alpha rhythms reveal when, where and how memories are retrieved. *BioRxiv*, 708602. https://doi.org/10.1101/708602

Miller, K. J., Sorensen, L. B., Ojemann, J. G., & Den Nijs, M. (2009). Power-law scaling in the brain surface electric potential. *PLoS Computational Biology*, *5*(12). https://doi.org/10.1371/journal.pcbi.1000609

Montgomery, S., & Buzsáki, G. (2007). Gamma oscillations dynamically couple hippocampal CA3 and CA1 regions during memory task performance. *Proceedings of the National Academy of Sciences*, *104*(36), 14495–14500.

Nyhus, E., & Curran, T. (2010). Functional role of gamma and theta oscillations in episodic memory. *Neuroscience and Biobehavioral*

bioRxiv preprint doi: https://doi.org/10.1101/2020.01.22.915330; this version posted January 23, 2020. The copyright holder for this preprint (which was not certified by peer review) is the author/funder, who has granted bioRxiv a license to display the preprint in perpetuity. It is made available under aCC-BY-NC-ND 4.0 International license.

Reviews, *34*(7), 1023–1035. https://doi.org/10.1016/j.neubiorev.2009.12.014

Oostenveld, R., Fries, P., Maris, E., & Schoffelen, J.-M. (2011). FieldTrip: Open source software for advanced analysis of MEG, EEG, and invasive electrophysiological data. *Computational Intelligence and Neuroscience*, *2011*, 1–9. https://doi.org/10.1155/2011/156869

Osipova, D., Takashima, A., Oostenveld, R., Fernandez, G., Maris, E., & Jensen, O. (2006). Theta and gamma oscillations predict encoding and retrieval of declarative memory. *Journal of Neuroscience*, *26*(28), 7523–7531. https://doi.org/10.1523/JNEUROSCI.1948-06.2006

Ruzich, E., Crespo-García, M., Dalal, S. S., & Schneiderman, J. F. (2019). Characterizing hippocampal dynamics with MEG: A systematic review and evidence-based guidelines. *Human Brain Mapping*, *40*(4), 1353–1375. https://doi.org/10.1002/hbm.24445

Sederberg, P. B., Schulze-Bonhage, A., Madsen, J. R., Bromfield, E. B., McCarthy, D. C., Brandt, A., … Kahana, M. J. (2007). Hippocampal and neocortical gamma oscillations predict memory formation in humans. *Cerebral Cortex*, *17*(5), 1190–1196. https://doi.org/10.1093/cercor/bhl030

Shannon, C. E., & Weaver, W. (1949). *A mathematical theory of communication*. Urbana, IL: University of Illinois Press.

Staresina, B. P., Michelmann, S., Bonnefond, M., Jensen, O., Axmacher, N., & Fell, J. (2016). Hippocampal pattern completion is linked to gamma power increases and alpha power decreases during recollection. *ELife*, *5*(AUGUST), 1–18. https://doi.org/10.7554/eLife.17397.001

Staudigl, T., & Hanslmayr, S. (2013). Theta oscillations at encoding mediate the context-dependent nature of human episodic memory. *Current Biology*, *23*(12), 1101–1106.

Tort, A. B. L., Komorowski, R., Eichenbaum, H., & Kopell, N. (2010). Measuring phase-amplitude coupling between neuronal oscillations of different frequencies. *Journal of Neurophysiology*, *104*(2), 1195–1210. https://doi.org/10.1152/jn.00106.2010

Tort, A. B. L., Komorowski, R. W., Manns, J. R., Kopell, N. J., & Eichenbaum, H. (2009). Theta-gamma coupling increases during the learning of item-context associations. *Proceedings of the National Academy of Sciences*, *106*(49), 20942–20947. https://doi.org/10.1073/pnas.0911331106

Tulving, E. (2002). Episodic memory: from mind to brain. *Annual Review of Psychology*, *53*, 1–25. https://doi.org/10.1146/annurev.psych.53.100901.135114

van Veen, B., van Drongelen, W., Yuchtman, M., & Suzuki, A. (1997). Localization of brain electrical activity via linearly constrained minimum variance spatial filtering. *IEEE Transactions on Biomedical Engineering*, *44*(9), 867–880. https://doi.org/10.1109/10.623056

Waldhauser, G. T., Braun, V., & Hanslmayr, S. (2016). Episodic memory retrieval functionally relies on very rapid reactivation of sensory information. *Journal of Neuroscience*, *36*(1), 251–260. https://doi.org/10.1523/JNEUROSCI.2101-15.2016

Zhang, H., & Jacobs, J. (2015). Traveling theta waves in the human hippocampus. *Journal of Neuroscience*, *35*(36), 12477–12487. https://doi.org/10.1523/JNEUROSCI.5102-14.2015